AIAA 80-1177R

Nonlinear Viscoelastic Design of Case-Bonded CMDB Grains

G. Meili,* G. Dubroca,* M. Pasquier,* and J. Thepenier*
Société Nationale des Poudres et Explosifs, Saint-Médard en Jalles, France

This paper discusses a method for the mechanical design of composite modified double base (CMDB) case-bonded grains subjected to thermal cycling. The proposed iterative method for stresses and margins of safety calculations takes into account the nonlinear viscoelastic behavior and compressibility of the propellant. The propellant behavior is derived from tensile testing. The nonlinearities mainly concern the modulus. The equations of equilibrium are numerically solved by sharing the grain web into many layers. The temperature, reduced time, nonlinear factor, Poisson's ratio, and damage (Farris's concept) are calculated at each step of time for each layer. Different grain shapes (star-shaped, wagon-wheel, finocyl inner bores) have been used in experiments with various types of thermal cycles. The comparison between prediction and experiment is acceptable even for a very complex strain-temperature history.

Nomenclature

a	= internal radius of a grain
b	= external radius of a grain
A_i, B_i	= coefficients of stress potential function
c, d	= nonlinearity function coefficients
D	= damage factor
E	= Young's modulus (general)
E_{tg}	= tangent modulus
E_r	= relaxation modulus
E_{at}	= reduced time modulus
em	= maximum strain
f	= viscoelasticity function
g	= nonlinearity function
K	= safety factor
K_t	= stress concentration factor
m	= exponent of maximum stress law
n	= exponent of relaxation modulus law
R	= traction rate
r	= radius (general)
Sm	= maximum stress
t	= current time
T	= temperature
V	= volume
X	= nonlinearity exponent
α	= thermal diffusivity
β	= volume change coefficient
ϵ	= strain
θ	= current temperature
σ	= stress
ρ	= volume change exponent

Subscripts

i	= layer number
r	= radial
z	= axial
c	= circumferential
0	= equivalent
∞	= infinite

Presented as Paper 80-1177 at the AIAA/SAE/ASME 16th Joint Propulsion Conference, Hartford, Conn., June 30-July 2, 1980; submitted Aug. 25, 1980; revision received March 2, 1981.

*Structural Analysis Engineer.

Introduction

A SIMPLE method was needed to design propellant grains in order to prevent damage from thermal cycling that occurs during service life. As typical tactical missile motors exhibit a high length-to-diameter ratio, the assumption of a semi-infinite cylinder is generally acceptable. Therefore, with classical grain shapes, analytical relationships lead to satisfactory mechanical and thermal calculations except for bond stresses near grain terminations. In this case, the problem is generally solved by a linear puddle, flaps, or stress-relief grooves. The highest-stress location is the inner contour of the grain. While with composite propellants an elastic approach to design is sufficient, CMDB propellants require more sophisticated calculations because of their high degree of nonlinear viscoelasticity.

The proposed method is reported and discussed in three steps. The first one is related to the experimental behavior of CMDB propellants, the second one to the calculation method of grain stresses, and the third one to the actual grain experiments.

Experimental Behavior

One classical approach to solve the problem of nonlinear viscoelasticity is to consider stresses as independent functions of time and strain.[1,2] It can be written

$$\sigma(t,\epsilon) = f(t) * g(\epsilon) \tag{1}$$

where * indicates that the operator is not strictly multiplicative.

At first, the time and strain function is determined; then, since failure data for safety factor calculations are required, Farris's damage concept[3-5] and multiaxial criterion parameters[6] will be evaluated. It is assumed that thermal stresses occurring in a grain during thermal cycling result from a succession of tensile loads; therefore experimental behavior is conducted only in tensile tests.

Time and Strain Function

The time function used here is the classical stress/relaxation modulus relationship established at several temperatures and small strains. According to Ref. 7, the relation used is (Fig. 1)

$$E_r = E(t)^{-n} \tag{2}$$

Tab-end tensile specimens were tested with the Instron Universal testing machine with its temperature conditioning system. The shift factors are calculated using the theory

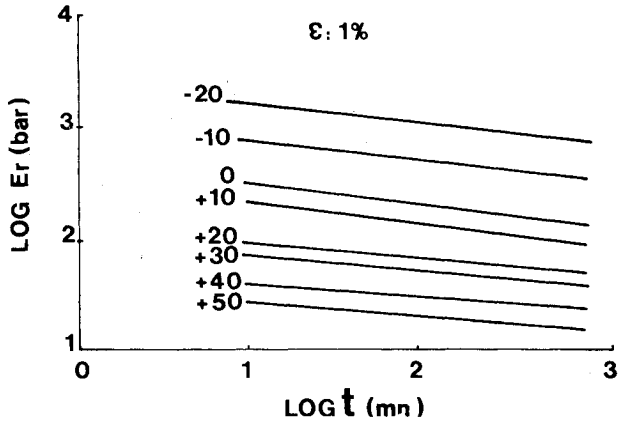

Fig. 1 Stress-relaxation modulus.

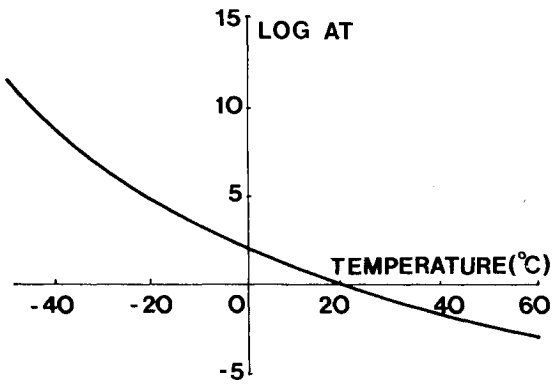

Fig. 2 Temperature-shift factor.

presented by Williams, Landel, and Ferry[8] (Fig. 2). The stress function is obtained from JANNAF tensile specimens tested at several constant temperatures and several strain rates. Stress-strain curves are normalized by the maximum stress and maximum strain at each step of time. Therefore,

$$\sigma/Sm = g(\epsilon/em)^{*}\epsilon \tag{3}$$

An example of this curve is shown in Fig. 3.

The function f is determined by stress-relaxation tests; the function g is given by the ratio of the tangent modulus to the secant modulus by dividing the stress-strain curve into approximately 20 steps. The different experimental results may be adjusted by

$$E_{tg}/E_{at} = c(\epsilon/em)^{X} + d \tag{4}$$

where em is the maximum strain at the given time and c and d are obtained by the classical parameters Sm and em.

It is obvious that g is not strictly independent of time because em is a function of the reduced time. This explains why Eq. (3) is not strictly multiplicative. Figure 4 shows the exponent X vs reduced time, while Fig. 5 is a plot of the tangent modulus vs reduced time.

Multiaxial Criterion

The effect of stress and strain on the failure prediction is taken into account by the use of the equivalent stress[6] defined by the maximum value of Eq. (5) or (6):

$$0.62\sqrt{(\sigma_\theta-\sigma_r)^2+(\sigma_r-\sigma_z)+(\sigma_z-\sigma_\theta)^2} \tag{5}$$

$$\frac{1}{17}(\sigma_\theta+\sigma_r+\sigma_z+\{(\sigma_r+\sigma_z+\sigma_\theta) + 128[(\sigma_\theta-\sigma_r)^2+(\sigma_r-\sigma_z)^2+(\sigma_z-\sigma_\theta)^2]\}^{1/2}) \tag{6}$$

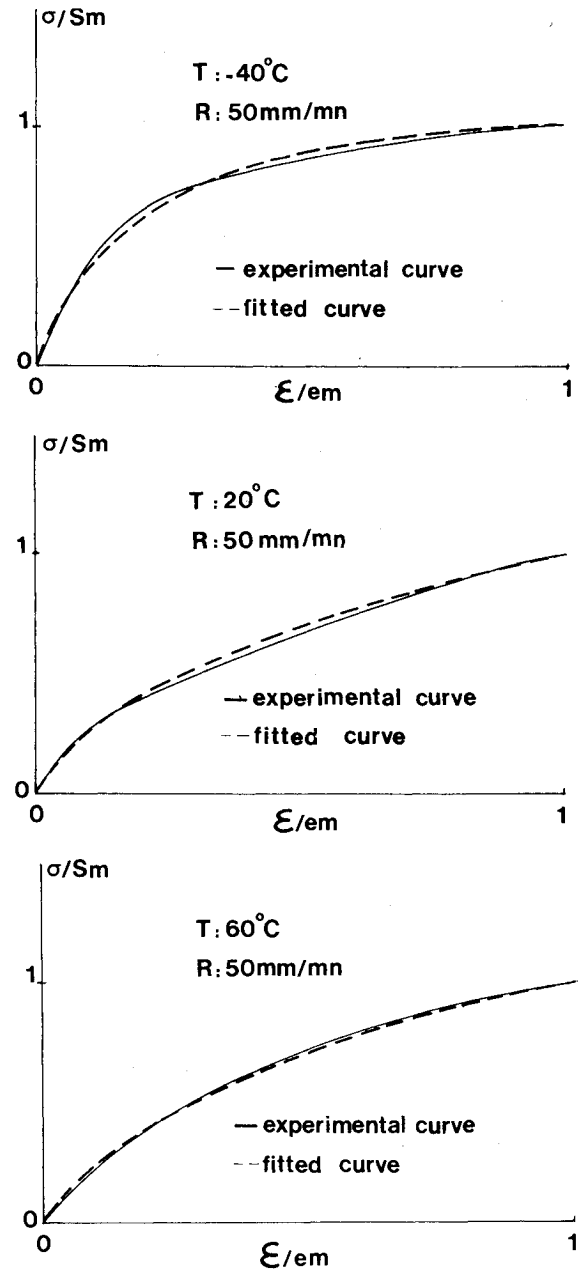

Fig. 3 Examples of stress-strain normalized curves.

The quantities are given in terms of the cylindrical components of stress. An equivalent strain may be defined by

$$\epsilon_0 = \sigma_0/E \tag{7}$$

Damage Concept

Because the temperature history of a propellant grain is not monotonic, the classical procedure is to consider a damage factor. The mathematical expression used for damage is[4,5]

$$D = k_1\|\sigma_0\|_\infty + k_2\|\sigma_0\|_m \tag{8}$$

$$\|\sigma_0\|_m = \left(\int_0^t \sigma_0^m dt\right)^{1/m} \qquad \|\sigma_0\|_\infty = \max\sigma_0$$

Then the safety factor is

$$K = 1/D \tag{9}$$

The validity of the mathematical expression of the damage concept was demonstrated on the maximum stress Sm for tensile tests (Fig. 6).

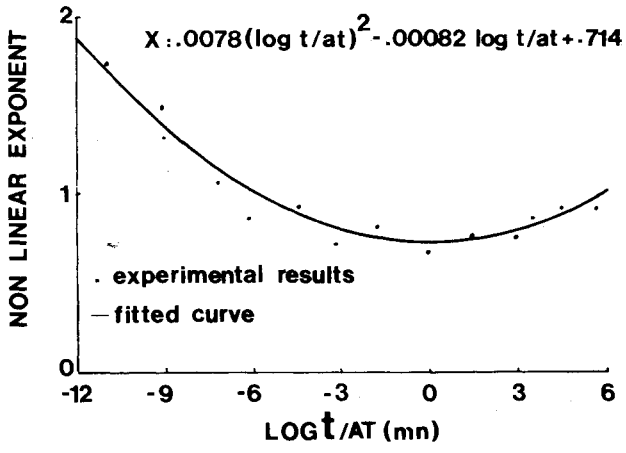

Fig. 4 Nonlinear exponent.

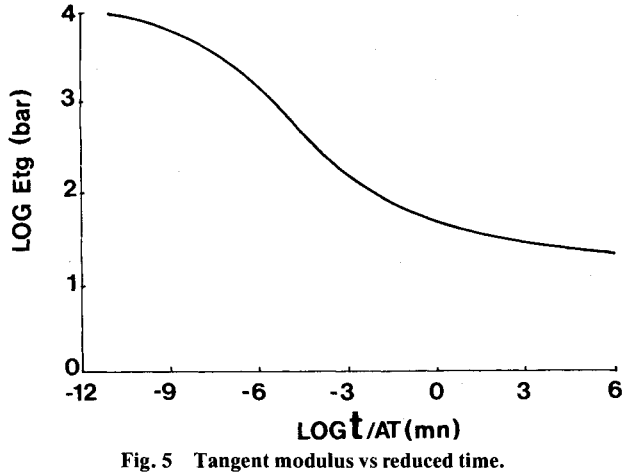

Fig. 5 Tangent modulus vs reduced time.

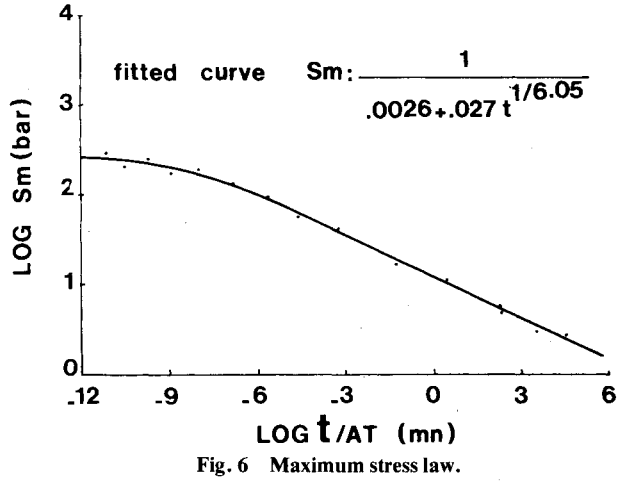

Fig. 6 Maximum stress law.

Propellant Compressibility

CMDB propellants exhibit a volume change when they are strained (Fig. 7). Tensile tests using a Farris dilatometer with tab-end specimens at different temperatures and strain rates were performed. It was found that the volume change can be expressed as

$$\Delta V/V=\beta(\epsilon/em)^{\rho} \tag{10}$$

This volume change results from a Poisson ratio variation. Assuming that the strains are quite small and the material is compressible, it may be written:

$$V=\tfrac{1}{2}(1-\Delta V/\epsilon V) \tag{11}$$

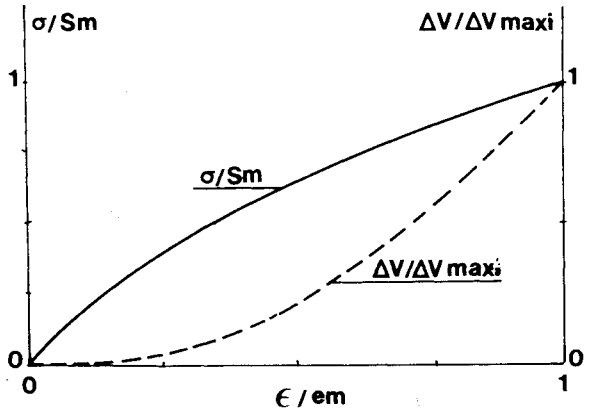

Fig. 7 Volume change.

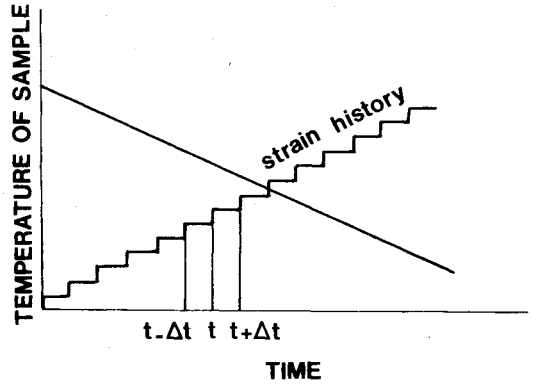

Fig. 8 Temperature and strain history of sample.

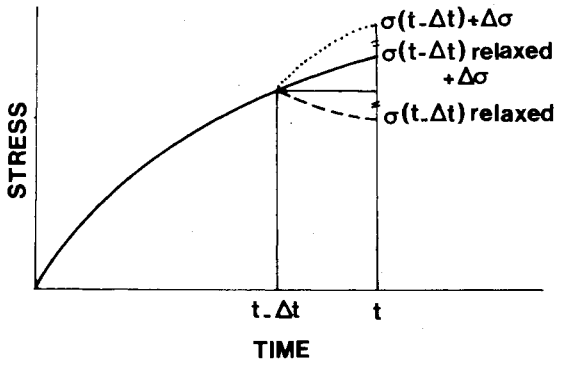

Fig. 9 Stress calculations for a sample.

Simultaneous Straining and Cooling

In order to determine the accuracy of the above approach, simultaneous straining and cooling of JANNAF specimens were performed. Stresses on samples were calculated by[9]

$$\sigma(t)=\sigma(t-\Delta t)_{\text{relaxed}}+\Delta\sigma \tag{12}$$

This equation is plotted in Figs. 8 and 9

using

$$\Delta\sigma=\Delta\epsilon\frac{\delta\sigma}{\delta\epsilon} \tag{13}$$

$\delta\sigma/\delta\epsilon$ is a modulus and therefore is obtained from the derivative of the stress-strain curve, by the derivative of

$$\sigma=\frac{E_{tg}}{c(\epsilon/em)^{x}+d} \tag{14}$$

The relaxation of stresses is taken into account only when the reduced time is increasing.

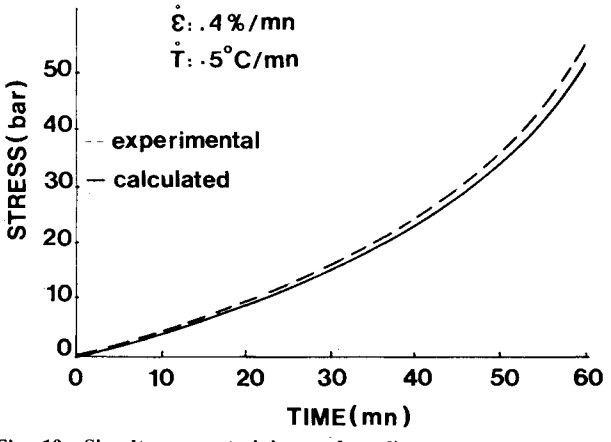

Fig. 10 Simultaneous straining and cooling stresses on JANNAF specimen.

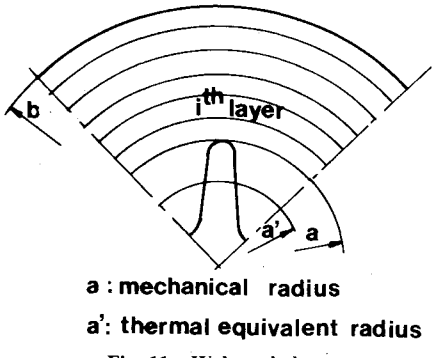

Fig. 11 Web-grain layers.

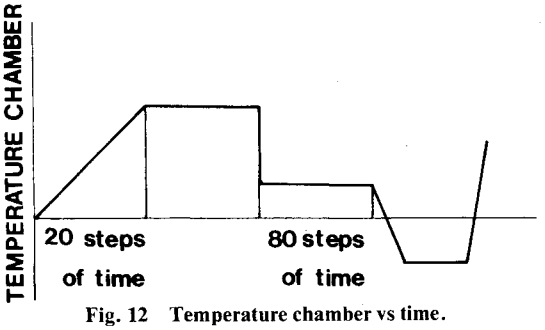

Fig. 12 Temperature chamber vs time.

The repetition of testing was fivefold, the temperature range was from 20 to $-10°C$, the strain changes were from 0 to 24%, the temperature change rate was 5°C/min, and the average linear coefficient of thermal contraction over the temperature change was 1.7×10^{-4} mm/°C. The comparison between calculated and experimental stresses is shown in Fig. 10. An acceptable agreement was found within 5%.

Grain stress calculations during thermal cycling require knowledge of the temperatures inside the grain. Fortunately both calculations of temperatures and stresses inside the grain can be analytically solved by dividing the grain into layers (Fig. 11).

Temperature Determination

In order to determine the temperature gradients inside the grain, the finite-difference method was applied to the layerd grain. It is assumed that the outside of the grain is subjected to a convective flow and the inner bore to none. The classical algorithm for temperature determination[10] is given by Eq. (15):

$$\theta_i(t+\Delta t)=\theta_i(t)+\alpha\Delta t\left[\frac{1}{\Delta x^2}(\theta_{i-1}-2\theta_i+\theta_{i+1})+\frac{1}{2r_i\Delta x}(\theta_{i+1}-\theta_{i-1})\right] \quad (15)$$

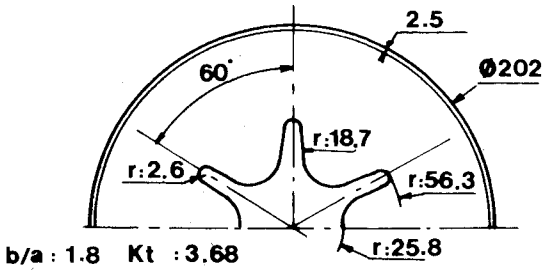

Fig. 13 Star grain.

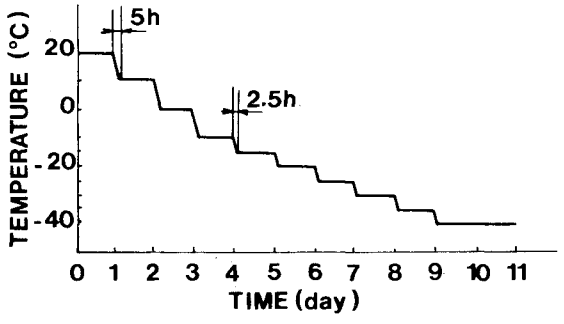

Fig. 14 Cycle 1.

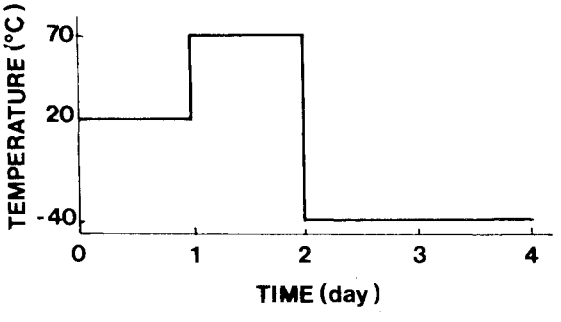

Fig. 15 Cycle 2.

where Δx is the layer thickness and Δt is the time interval. With a heat-exchange coefficient of 10 $W/m^2/°C$, this method gives an acceptable temperature prediction within 2%.

Grain Stress Calculations

It is assumed that for each layer the mathematical expression of stress is

$$\sigma_{r_i}\theta_i=A_i\pm B_i/r^2 \quad (16)$$

The conditions at the limits are that $\sigma_r=0$ at the inner bore and $\epsilon_\theta=0$ at liner case interface. The continuity of ϵ_θ and σ_r between each layer is assumed. Therefore Eqs. (11-14) are used for each layer and the equivalent strain is employed. The $\Delta\sigma$ for each step of time and for each layer is obtained by the solution of a $2n$ system of linear equations (n is the number of layers).

Because the resultant strain is a function of temperature, modulus, and volume change, iterations were required. Iterations were run on the equivalent strain until the error between two iterations is less than 10^{-5}. To perform such an analysis on the grains, 20 layers were required. Each period of thermal cycles was divided into 20 or 80 steps of time (Fig. 12). The duration of calculations for each period was about 3 min on a UNIVAC 1106 computer. After determination of the stresses for each layer, Eqs. (8) and (9) give the safety factor. When the inner bore is star-shaped, the classical stress-concentration factor was introduced. New iterations on the equivalent strain are required for the inner layer only.

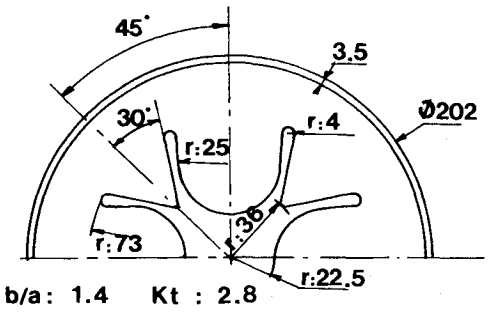

Fig. 16 Wagon-wheel grain.

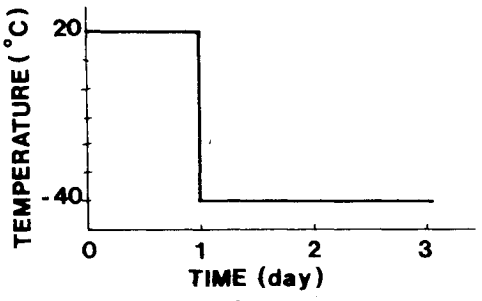

Fig. 17 Cycle 3.

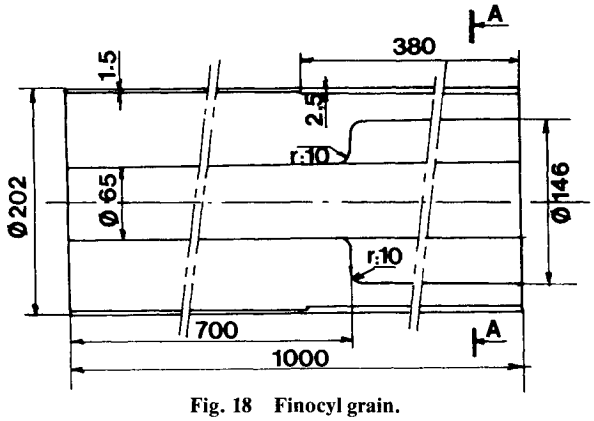

Fig. 18 Finocyl grain.

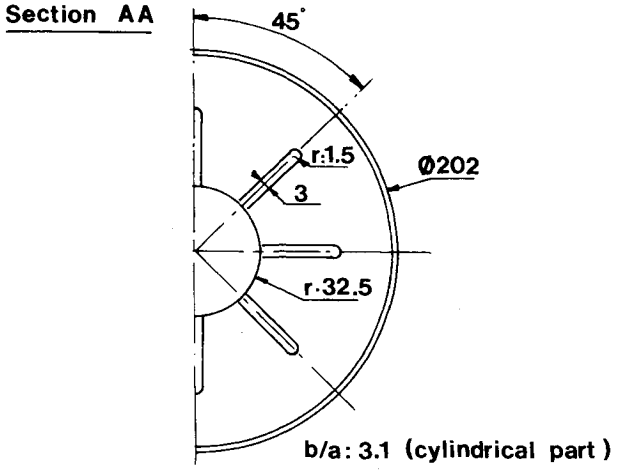

Fig. 19 Finocyl grain (section AA).

Experiments on Grains

The method developed above was applied to a motor configuration with a heavy-wall steel case in which the propellant was cured at 60°C. The length of the motor was 1 m, the inside diameter of the motor case was 0.202 m, and the ends were free. Prior to propellant casting, each case was coated with a 2-mm thick liner.

Table 1 Predicted safety factors compared to experimental results

		Predicted	Observations	Linear predictions
Star grain	cycle 1	0.9	failure	0.6
	cycle 2	1.1	no failure	0.2
Wagon wheel	cycle 1	1.6	no failure	1.3
	cycle 3	1.7	no failure	0.8
Finocyl	cycle 1	1.3	no failure	0.7

For inner-bore stress calculations it was assumed that the mechanical properties of the linear are the same as those of the propellant. Before cycling, the motors were X-rayed and endoscoped. This procedure was repeated after each period of thermal cycling while endoscopy was continuously conducted. The thermal cycles were initiated one month after grain-curing termination. During this waiting period, the motor was stored at 20°C ± 1°C with a 30% relative humidity.

The thermal cycles applied on the star grain (Fig. 13) are shown in Figs. 14 and 15. The thermal cycles applied on the wagon-wheel grain (Fig. 16) are shown in Figs. 14 and 17. The finocyl grain is described in Figs. 18 and 19. The inner-bore geometry is such that the end-effect on the cylindrical portion of the inner bore lowers stresses about 20%. This grain was only submitted to the type-1 thermal cycle.

Results

Table 1 shows the different predicted safety factors and compares them to the experimental results. For the type-1 cycle, the predicted failure of the star grain experimentally occurs at −38°C ± 1°C. The last column shows the safety factors obtained by the classical linear procedure.

Conclusion

A numerical procedure for grain design has been described which involves nonlinear viscoelasticity and compressibility of the propellant. The conducted experiments support the validity of such a method; they show an acceptable agreement between prediction and experiment, both on samples (straining and cooling) and on actual motors of various configurations. These experiments show the inadequacy of the elastic method to predict motor failure with CMDB propellant grains. The developed procedure is to be used for the design of case-bonded grains whenever the nonlinear viscoelasticity of the propellant is significant.

References

[1] Francis, F.C. and Carlton, C.H., "Some Aspects of Nonlinear Mechanical Behavior of a Composite Propellant," *Journal of Spacecraft and Rockets,* Vol. 6, No. 1, 1969, pp. 65-69.

[2] Lindsey C.H. and Woods, J.E., "Determination of Dewetting Criterion for Nonlinear Solid Propellants Stress Analysis," *Journal of Engineering Materials and Technology,* July 1975, pp. 271-274.

[3] Farris, R.J. and Schapery, R.A., "Development of a Solid Rocket Propellant Nonlinear Viscoelastic Constitutive Theory," Aerojet Reports, AD 769263 and AD 769264, June 1973.

[4] Farris, R.J., Herrmann, L.R., Hutchinson, J.R., and Schapery, R.A., Aerojet final report, AD-A012213, May 1975.

[5] Bills, V.W., "Applications of Nonlinear Viscoelasticity and Cumulative Damage," Aerojet Report, 1565-26-Q-1, July 1970.

[6] Von Mises, R., "Göllinger Nachrichter," *Mathematische Physikalische K.,* 1913, p. 582.

[7] *ICRPG Solid Propellant Mechanical Behavior Manual,* CPIA publication, The Johns Hopkins University, Silver Spring, Md., Sec. 2-3-46, Sept. 1963.

[8] Williams, M.L., Landel, R.F., and Ferry, J.D., "The Temperature Dependance of Relaxation Mechanism in Amorphous Polymers and Other Glass Forming Liquids," *Journal of the American Chemical Society,* Vol. 77, 1955, pp. 3701-3707.

[9] More, F.C., Robinson, C.N., and Graham, P.M., "Response of Viscoelastic Media During Changing Temperature," AIAA Paper 68-511, June 1968.

[10] Carslaw, H.S. and Jaeger, J.C., *Conduction of Heat in Solid,* 2nd ed., Oxford University Press, London, 1959, pp. 466-478.